

Presented at Japanese Electronic Ceramic  
Seminar, Kamakura, Japan,  
March 22 - 23, 1974

LBL-3101

SINTERING MECHANISMS IN PZT

Richard M. Fulrath

March 1974

Prepared for the U. S. Atomic Energy Commission  
under Contract W-7405-ENG-48

TWO-WEEK LOAN COPY

*This is a Library Circulating Copy  
which may be borrowed for two weeks.  
For a personal retention copy, call  
Tech. Info. Division, Ext. 5545*



LBL-3101  
c. j.

## **DISCLAIMER**

This document was prepared as an account of work sponsored by the United States Government. While this document is believed to contain correct information, neither the United States Government nor any agency thereof, nor the Regents of the University of California, nor any of their employees, makes any warranty, express or implied, or assumes any legal responsibility for the accuracy, completeness, or usefulness of any information, apparatus, product, or process disclosed, or represents that its use would not infringe privately owned rights. Reference herein to any specific commercial product, process, or service by its trade name, trademark, manufacturer, or otherwise, does not necessarily constitute or imply its endorsement, recommendation, or favoring by the United States Government or any agency thereof, or the Regents of the University of California. The views and opinions of authors expressed herein do not necessarily state or reflect those of the United States Government or any agency thereof or the Regents of the University of California.

## Sintering Mechanisms in PZT

Richard M. Fulrath

Department of Materials Science and Engineering,  
College of Engineering, and Inorganic Materials  
Research Division, Lawrence Berkeley Laboratory,  
University of California, Berkeley

### Introduction

The sintering process for lead zirconate titanate ceramics is one of the most complex encountered in the ceramic material area. First, the system shows an unusually wide range of intrinsic non-stoichiometry at high temperatures. Secondly, the volatile nature of PbO makes high temperature processing difficult. Lastly, small amounts of impurities can cause drastic changes in the ferroelectric or piezoelectric properties. This discussion will concentrate on the sintering of a few selected PZT compositions which include the basic PZT compound and various dopants. We will concentrate on conventional sintering practice and not include hot pressing.

### Crystal Structure of PZT

Above the Curie temperature and below the liquidous temperature lead titanate and lead zirconate form a complete solid solution with the cubic perovskite ( $\text{CaTiO}_3$ ) structure. Upon liquid formation the system decomposes into 2 crystalline phases and a lead rich liquid<sup>(1)</sup>; therefore, the incongruent nature of melting makes the system a pseudo-binary.

The structure of PZT can be visualized by face center cubic packing oxygen ions and replacing the corner ions with lead ions of +2 charge and filling the central octahedral

hole with either +4 zirconium or titanium ions. The 12-fold coordinated hole occupied by the lead 2+ ion has an ionic radius of oxygen, 1.40Å. The best value for the ionic radius of Pb<sup>2+</sup> is 1.20Å. Therefore, some lattice distortion is introduced by the lead ion filling the hole. Similarly the central octahedral hole is too large for Ti<sup>4+</sup>, 0.605Å, and close to the size of the Zr<sup>4+</sup>, 0.72Å. (2)

The interstitial sites in the structure, 12 octahedral holes on the cube edges and 8 tetrahedral holes at the (1/4, 1/4, 1/4) positions, are unlikely to be filled, because each has both positive and negative ion neighbors. (3)

#### High Temperature Intrinsic Non-Stoichiometry

At high temperatures the PbTiO<sub>3</sub>, PbZrO<sub>3</sub> and solid solution mixtures show a wide solid solution region. Fig. 1 shows the three component phase equilibrium diagram for the PbO - ZrO<sub>2</sub> - TiO<sub>2</sub> at 1100°C. The solid solution region is a result of recent work. (4) Fig. 2 gives the PbO activity as a function of reciprocal temperature for PbTiO<sub>3</sub>, PbZrO<sub>3</sub> and Pb(Ti<sub>0.5</sub>Zr<sub>0.5</sub>)O<sub>3</sub> at the limits of the solid solution region. The vapor pressure of PbO above liquid or crystalline PbO at the specific temperature was taken as the standard state. If a Pb(Zr<sub>0.5</sub>Ti<sub>0.5</sub>)O<sub>3</sub> green ceramic was heated to a given temperature in a sealed container containing a mixture of PbZrO<sub>3</sub> and ZrO<sub>2</sub> to provide a PbO atmosphere, the sample would equilibrate with the atmosphere and develop an intrinsic vacancy concentration of both Pb and O vacancies to give a composition Pb<sub>1-x</sub>V<sub>pb\_x</sub>(Ti<sub>0.5</sub>Zr<sub>0.5</sub>)O<sub>3-x</sub>V<sub>o\_x</sub>.

Therefore, the composition of a packing powder around a PZT can control the intrinsic defect structure.

#### Extrinsic Defects

PZT can be doped with the Pb or O ions on its charge sites. A strong influence through its structure and La<sup>3+</sup> on the Pb<sup>2+</sup> vacancies oxygen vacancies limit or is in distribution on the electrode liquid film at boundaries. insoluble in behaves in the have high potential grain boundaries for the ceramic ferroelectric

#### Sintering Studies

Al<sub>2</sub>O<sub>3</sub> and into PZT with ing the calcining pebbles. The identify the Ti and 0.4 Zr milled in organic Al(NO<sub>3</sub>)<sub>3</sub> or fired under

### Extrinsic Defect Structure and Second Phases

PZT can be doped with various ions to form vacancies on the Pb or O site. The affect of an individual ion will depend on its charge and ionic size. The defect produced will have a strong influence on the piezo and ferroelectric properties through its interaction with the ferroelectric domains.  $\text{Bi}^{3+}$  and  $\text{La}^{3+}$  on the  $\text{Pb}^{2+}$  site and  $\text{Nb}^{5+}$  on the  $\text{Ti}^{4+}$  site can produce  $\text{Pb}^{2+}$  vacancies.  $\text{Sc}^{3+}$  or  $\text{Al}^{3+}$  on the  $\text{Ti}^{4+}$  site can produce oxygen vacancies. When an element is added above the solubility limit or is insoluble, secondary phases will be produced. The distribution of the secondary phase can have a strong influence on the electrical properties, especially if it is present as a liquid film at high temperatures which encompasses all grain boundaries. A simple model is shown in Fig. 3.  $\text{SiO}_2$  which is insoluble in PZT because of the ionic size of  $\text{Si}^{4+}$  ( $0.42\text{\AA}$ ) behaves in this fashion and causes applied electric fields to have high potential drops across the low dielectric constant grain boundary phase. This causes an indicated increase in  $E_c$  for the ceramic, because the potential gradient across the ferroelectric phase is reduced. (5)

### Sintering Studies

$\text{Al}_2\text{O}_3$  and  $\text{SiO}_2$  are two impurities which can be introduced into PZT either in mixing the primary raw materials or grinding the calcined composition in alumina jars with alumina pebbles. Therefore, one of the first studies (6) should be to identify their affect on sintering. A PZT composition of 0.6 Ti and 0.4 Zr prepared from high purity chemicals and mixed or milled in organic materials had various percentages of either  $\text{Al}(\text{NO}_3)_3$  or colloidal  $\text{SiO}_2$  added. Samples were prepared and fired under a controlled  $\text{PbO}$  atmosphere for 1 1/2 hours at

1210 C. As can be seen in Fig. 4 both additives lead to increased densification when their addition exceeds a minimum amount.

A further study of the sintering of PZT included the use of dopants and  $\text{SiO}_2$  and  $\text{Al}_2\text{O}_3$  additives. (5)  $\text{Bi}^{3+}$  and  $\text{Nb}^{5+}$ , both dopants which should favor Pb vacancy production, were used.  $\text{Bi}^{3+}$  and  $\text{Nb}^{5+}$  were added at 0.02 atomic percent, whereas, alumina and silica were added as 0.4 weight percent additions. All samples were presintered at 800 C for one hour to remove organic materials and increase the green strength. The specimens were fired in a packing powder of the same composition of the samples  $\text{Pb}(\text{Ti}_{0.47}\text{Zr}_{0.53})\text{O}_3$  that was on the high PbO activity side of the solid solution. The firing geometry is shown in Fig. 5. The specimens were fired in one atmosphere oxygen. The furnace was raised to 1200°C at 300°C/hr and held for the required time. The initial density was determined after 20 minutes at 1200°C and is shown in Fig. 6. As shown in the figure,  $\text{SiO}_2$  additions increase the initial density in the undoped and doped samples; whereas, alumina additions decrease the initial density. On holding the sample at temperature the density increase for samples with no alumina or silica additives was linear with time<sup>1/2</sup>. When either alumina or silica were present a time<sup>1/3</sup> relation was observed. The sintering behaviour is shown in Fig. 7, 8, and 9. With no dopants,  $\text{Bi}^{3+}$ , or  $\text{Nb}^{5+}$  dopants and no silica or alumina a solid state diffusion process was apparently followed. When  $\text{Al}^{3+}$  or  $\text{Si}^{4+}$  were present a liquid phase sintering was encountered as shown by the  $t^{1/3}$  dependence.

Alumina additions markedly reduced ferroelectric behaviour, as shown in Fig. 10.  $\text{Nb}^{5+}$  developed square loops and could compensate for  $\text{Al}^{3+}$ .

Silica  
uration pol  
both lead v  
action.

Alumin  
electric pr  
and as grai  
Alumina and  
grain bound  
was decreas  
defect pair

The ra  
purity PZT  
shown in Fi

Fig. 1  
rate for Nb  
erial has  
of equal a  
densificat  
alone give  
through co  
diffusion  
rates for  
in the den  
boundary d

#### Summary

Sinte  
and atmo  
with the d  
Lattice de

Silica additions increased  $E_c$  without changing the saturation polarization significantly (Fig. 11).  $Nb^{5+}$  and  $Bi^{3+}$ , both lead vacancy generators, were interchangeable in their action.

Aluminum and niobium were self compensating in ferroelectric properties as shown in Fig. 10 and also in sintering and as grain growth inhibitors as shown in Fig. 12.<sup>(3)</sup> Both Alumina and niobium increased grain boundary drag and impeded grain boundary mobility. When both were present their action was decreased due to association of  $Al^{3+}$  and  $Nb^{5+}$  to form defect pairs without O or Pb charged vacancies.

The rate determining species in sintering undoped high purity PZT was determined to be the oxygen vacancy from the data shown in Fig. 13.

Fig. 14 compares the grain size compensated densification rate for Nb, Al, Nb + Al, and undoped material. Undoped material has the highest densification rate while the mixed doping of equal atomic percents of Nb and Al give nearly the same densification rate at an equivalent grain size. Nb and Al doping alone give lower densification rates but lead to a higher density through control of grain growth and subsequent reduction of the diffusion path length (Fig. 12). The nonlinear densification rates for Al and Nb doped materials may be due to a change in the densification mechanism from volume diffusion to grain boundary diffusion.

#### Summary

Sintering of PZT requires that the impurities, dopants, and atmosphere be carefully controlled to produce materials with the desired ferroelectric or piezoelectric properties. Lattice defects whether intrinsic or extrinsic play an im-

portant role on sintering and electrical properties.

Acknowledgements

This work was done under the auspices of the U.S. Atomic Energy Commission.

References

1. R. L. Moon and R. M. Fulrath, J. Am. Ceramic Soc., 54 124 - 125 (1971).
2. R. B. Atkin, R. L. Holman, and R. M. Fulrath, J. Am. Ceramic Soc., 54 113 - 115 (1971).
3. R. B. Holman and R. M. Fulrath, J. Am. Ceramic Soc., 54 265 - 270 (1971)
4. R. L. Holman and R. M. Fulrath, J. Applied Physics, Dec. (1973).
5. R. B. Atkin and R. M. Fulrath, Interfaces Conference, Edited by R. C. Gifkins, Butterworth and Co., Sydney, 185 - 207 (1969).
6. G. A. Pryor, M. S. Thesis, University of California, May (1968).

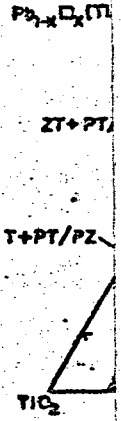


Fig. 1 Ternary

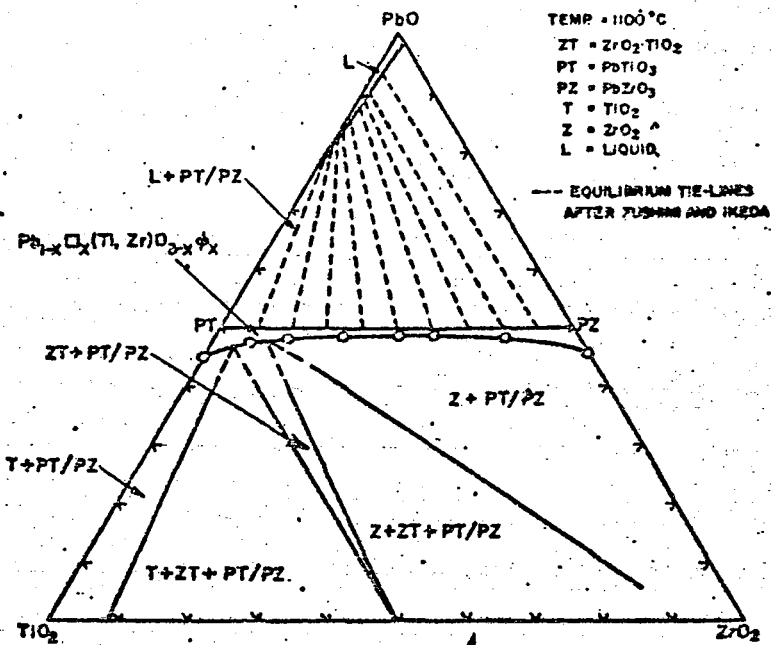


Fig. 1 Ternary phase diagram of PbO - ZrO<sub>2</sub> - TiO<sub>2</sub> at 1100°C.

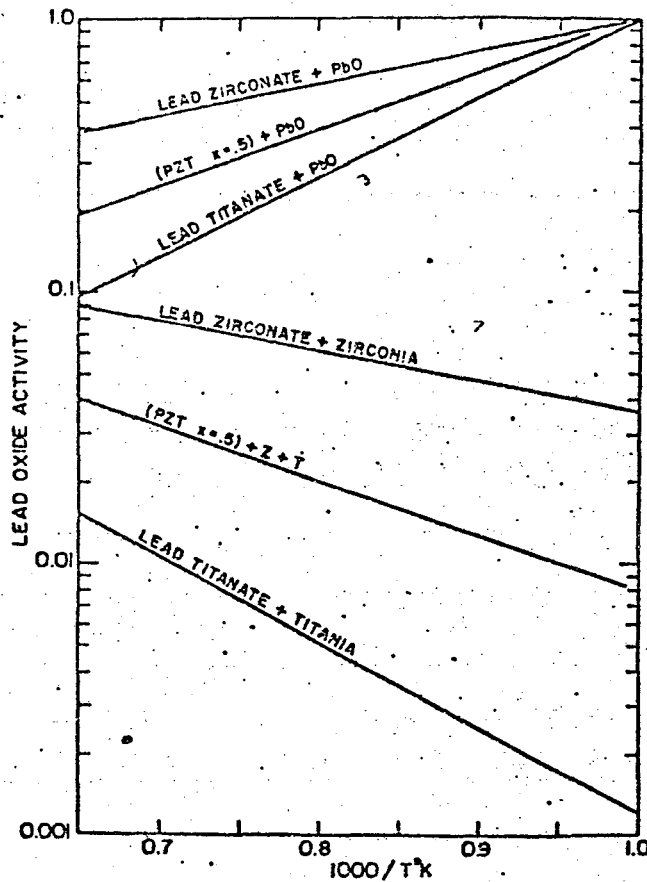


Fig. 2 PbO activity as a function of reciprocal temperature for three selected compositions.

$$a_{\text{PbO}} = \frac{\text{Pressure of PbO above the system}}{\text{Pressure of PbO above liquid or solid PbO}}$$

Fig. 3 Phy  
a c

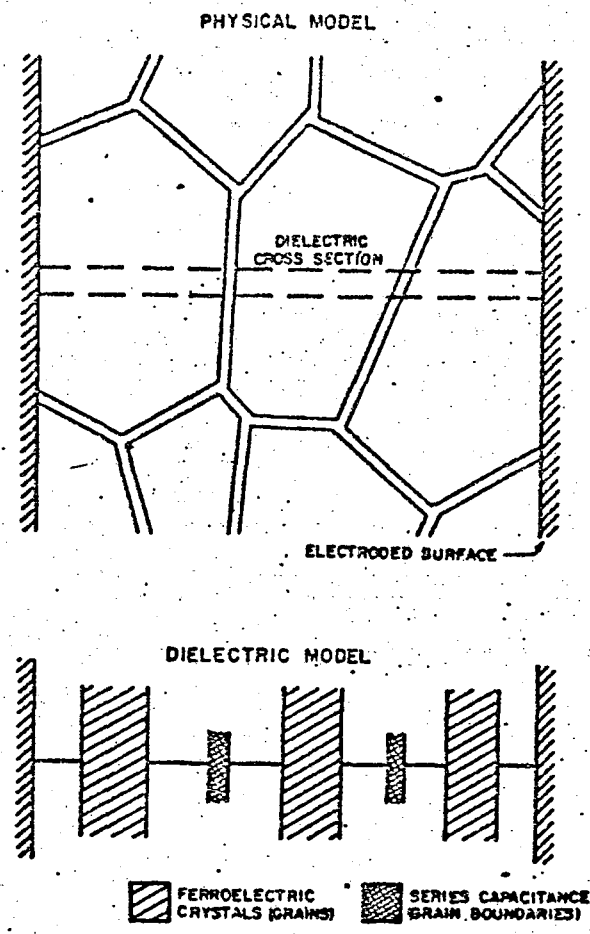


Fig. 3 Physical and dielectric model for a ferroelectric with a continuous grain boundary phase.

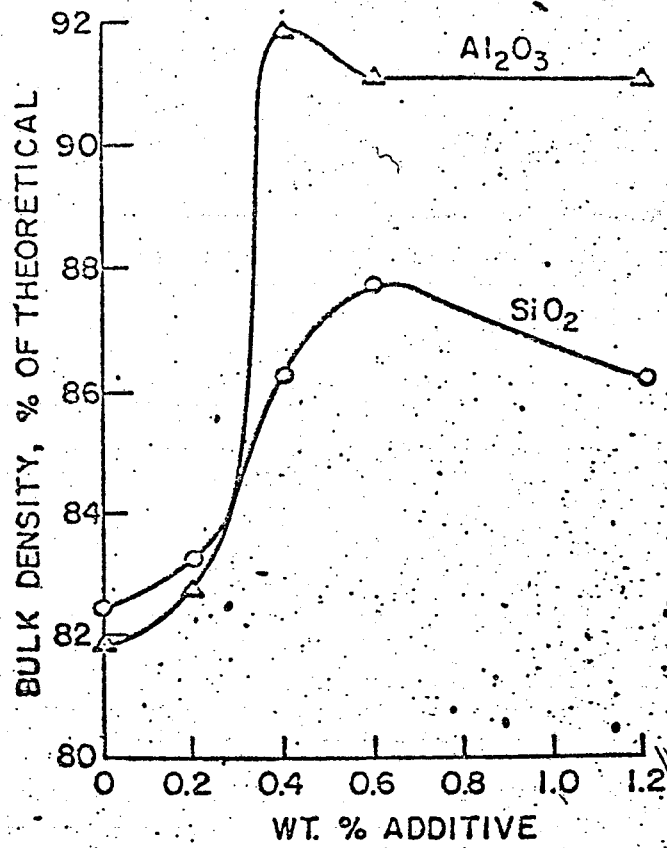


Fig. 4 The effect of Al<sub>2</sub>O<sub>3</sub> and SiO<sub>2</sub> additions to Pb(Zr<sub>0.4</sub>Th<sub>0.6</sub>)O<sub>3</sub> on the sintered density. 1 1/2 hours at 1210°C.

Fig. 5 Geo  
pre

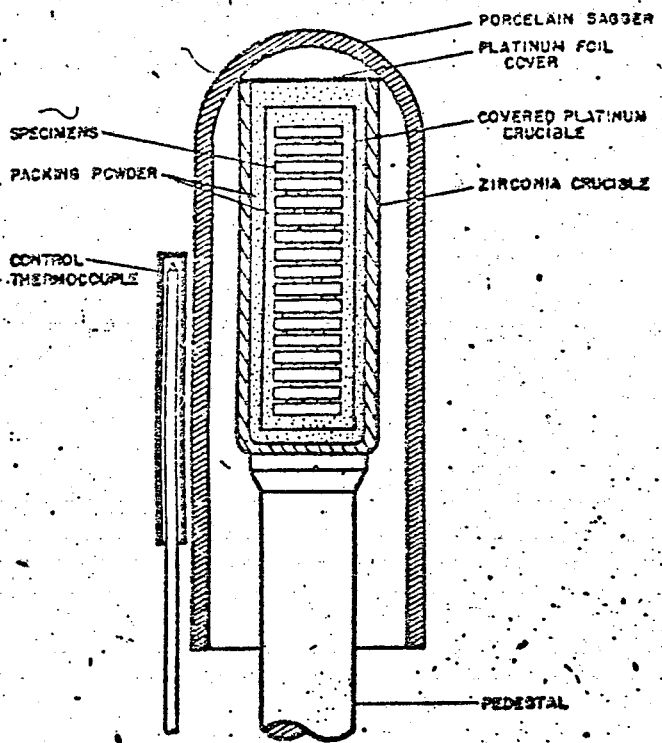


Fig. 5 Geometry for sintering studies to control the PbO vapor pressure.

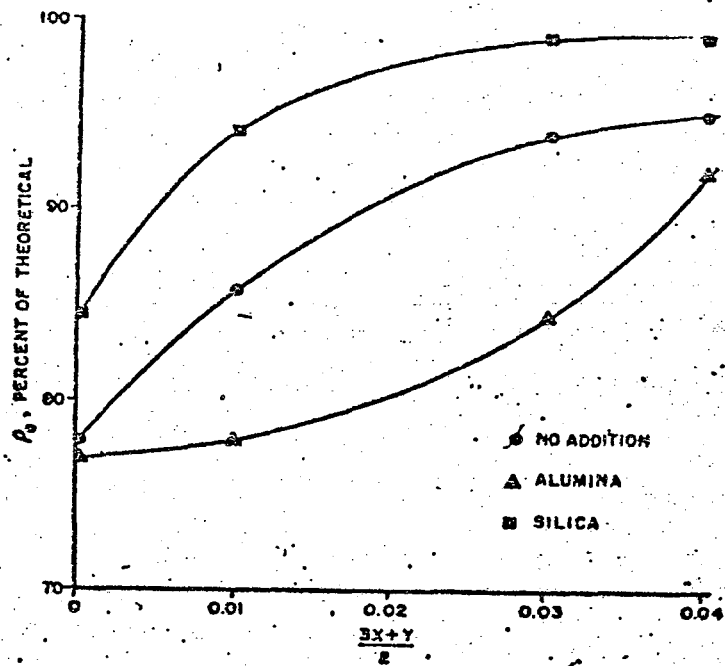


Fig. 6 The initial density after 20 minutes at 1200°C for  $\text{Pb}(\text{Ti}_{0.47}\text{Zr}_{0.53})\text{O}_3$  plus additions ( $\text{SiO}_2$  or  $\text{Al}_2\text{O}_3$  at 0.4 weight percent) or dopants ( $\text{Nb}^{5+}$  or  $\text{Bi}^{3+}$  at 0.02 atomic percent) or both. 0 refers to no dopant, 0.01 is 0.02 atomic percent  $\text{Nb}^{5+}$ , 0.03 is 0.02 atomic percent  $\text{Bi}^{3+}$ , and 0.04 is 0.02 atomic percent each of  $\text{Bi}^{3+}$  and  $\text{Nb}^{5+}$ .

Fig. 7

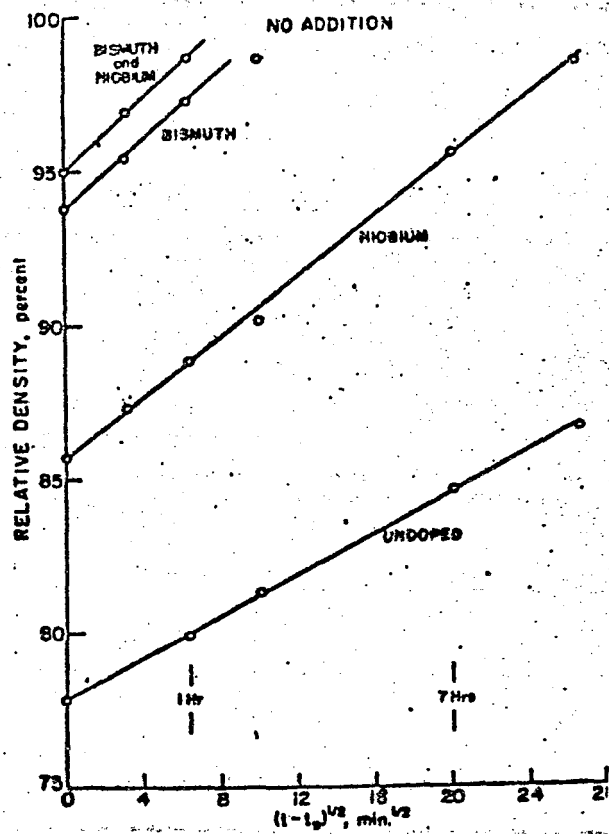


Fig.7 Density vs. reduced time for isothermal sintering with no additives.

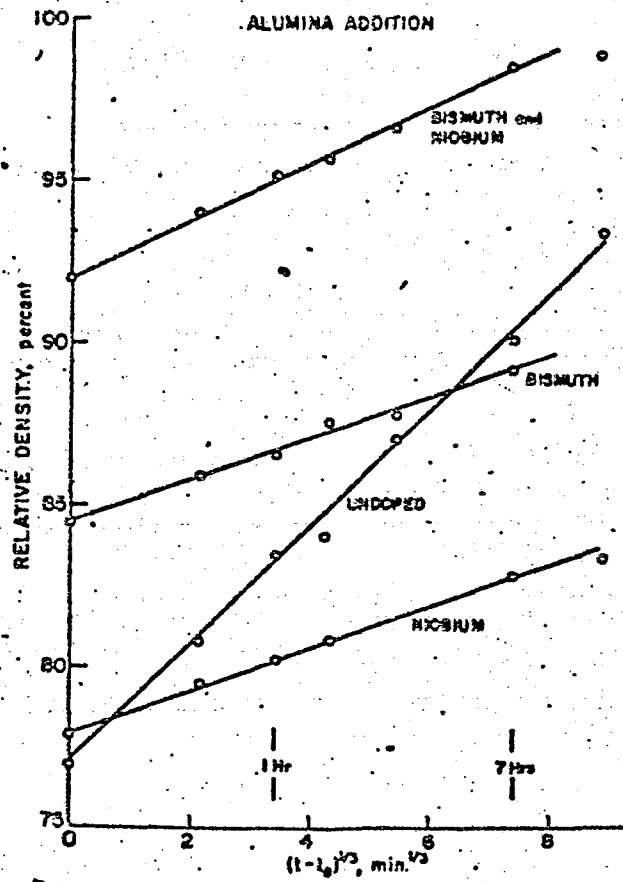


Fig.8 Density vs. reduced time for isothermal sintering with an alumina addition.

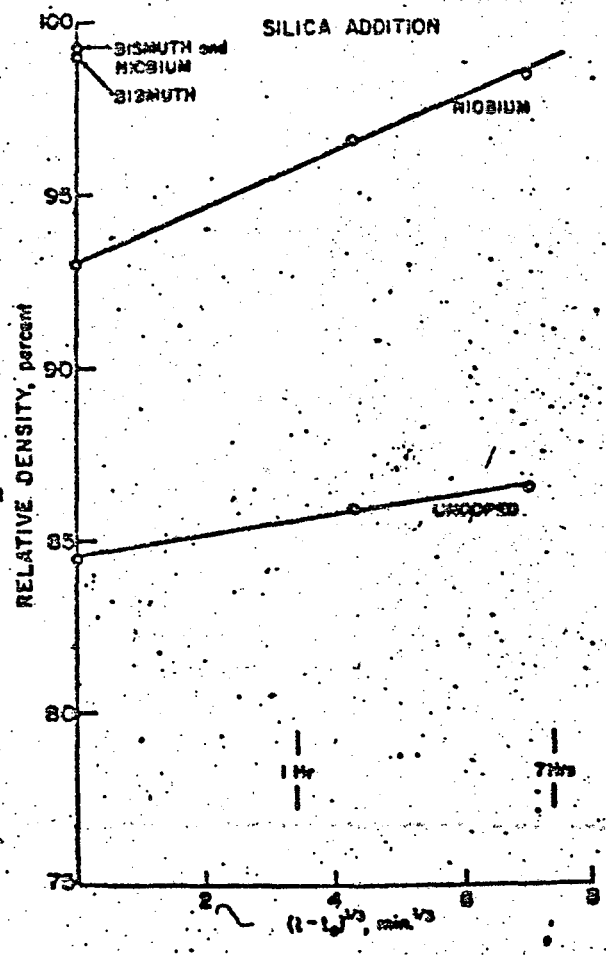


Fig. 9 Density vs. reduced time for isothermal sintering with a silica addition.

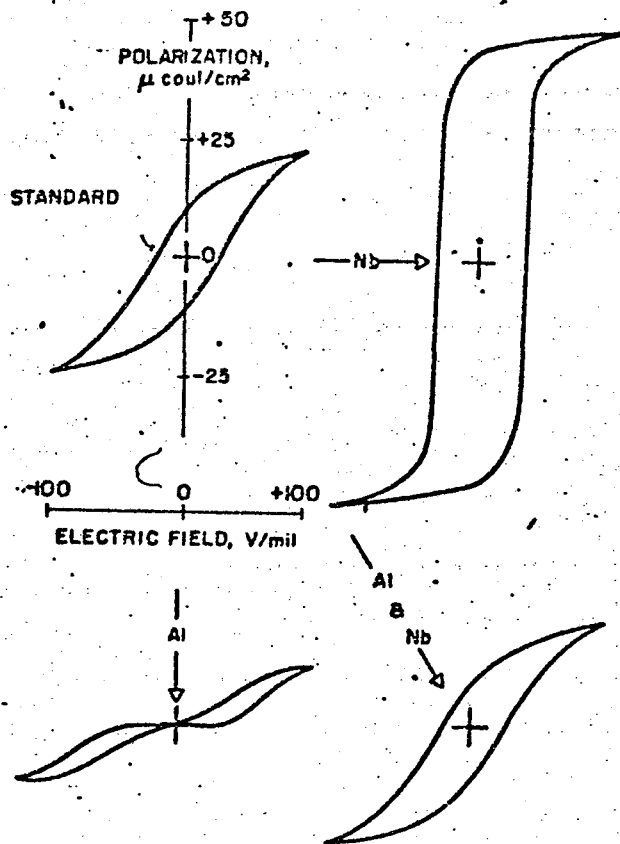
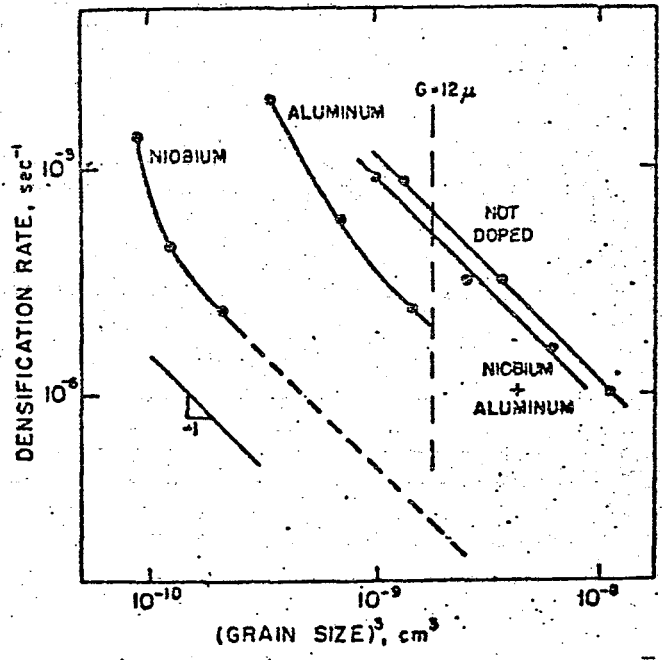


Fig.10 Typical ferroelectric loops for Nb<sup>5+</sup> and Al<sup>3+</sup> modified material.

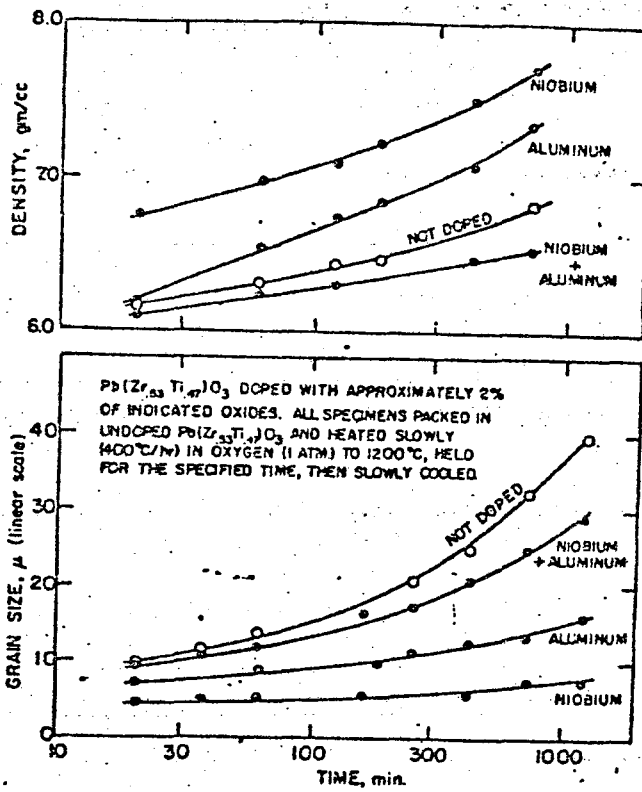
Fig.14 D

DENSIFICATION RATE, sec<sup>-1</sup>



XIII 707-4396

Fig. 14 Densification rate vs. grain size for undoped and doped PZT compositions.



XBL 707-6588

Fig.12 Density and grain size vs. sintering time for  $Al^{3+}$  and  $Nb^{5+}$  modified PZT compared to high purity material.

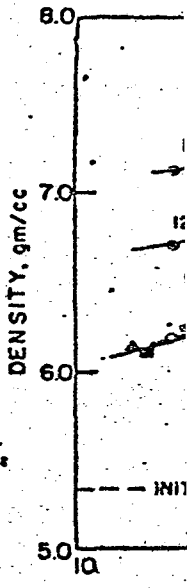


Fig.1

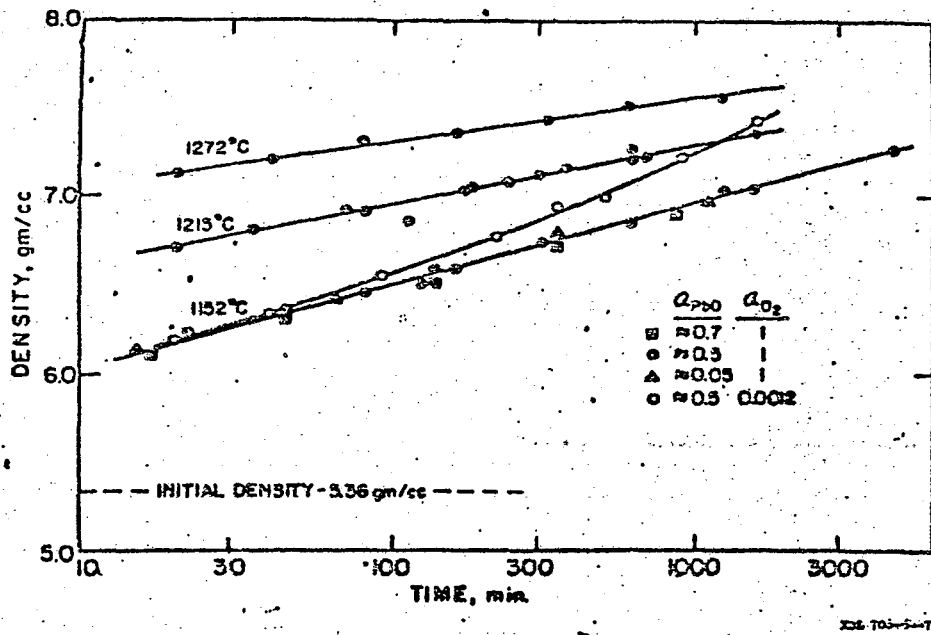


Fig.13 Sintering behaviour of high purity PZT in controlled activity environments.

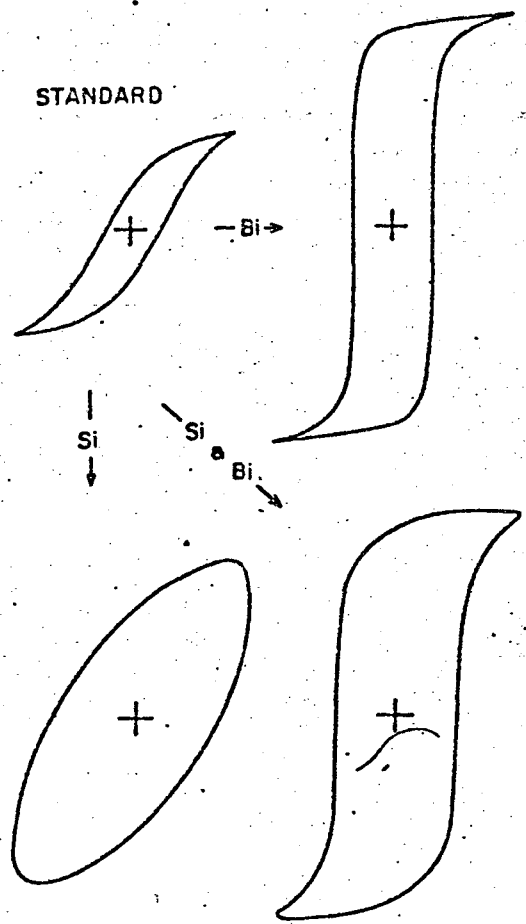


Fig.11 Typical ferroelectric loops for Bi<sup>3+</sup> and SiO<sub>2</sub> modified material ( see Fig.3 ).

LEGAL NOTICE

*This report was prepared as an account of work sponsored by the United States Government. Neither the United States nor the United States Atomic Energy Commission, nor any of their employees, nor any of their contractors, subcontractors, or their employees, makes any warranty, express or implied, or assumes any legal liability or responsibility for the accuracy, completeness or usefulness of any information, apparatus, product or process disclosed, or represents that its use would not infringe privately owned rights.*

TECHNICAL INFORMATION DIVISION  
LAWRENCE BERKELEY LABORATORY  
UNIVERSITY OF CALIFORNIA  
BERKELEY, CALIFORNIA 94720